6th Australasian Hydraulics and
Fluid Mechanics Conference
Adelaide, Australia, 5-9 December 1977

A Finite Element Frozen Vorticity Solution for Two-dimensional Wind Flow over Hills

R. J. ASTLEY

Lecturer, Department of Mechanical Engineering, University of Canterbury, Christchurch, N.Z.

SUMMARY A method is presented for predicting the mean wind flow over low hills. The finite element method is used in conjunction with a frozen vorticity assumption. Computed results for a number of simple escarpments compare well with measured data from wind tunnel models and field tests.

1 INTRODUCTION

It is well known that wind speeds above hills may be much larger than those at equivalent heights above flat ground. This phenomenon results from the action of two non-linear mechanisms represented in the equations of motion by the convective terms and the turbulent Reynolds stress terms. The Reynolds stress terms are particularly difficult to model mathematically as a closure assumption is required to relate them to the mean flow variables. For uniform flow a commonly used closure assumption is derived from Prandtl's mixing length hypothesis and results in the familiar log profile for the mean horizontal velocity. Such a profile can be matched well to existing data for wind flow over level ground, subject to the choice of a suitable 'roughness length' y_o. y_o is found empirically to be of the order of one tenth of the height of the local roughness elements of the underlying terrain. (ESDU, 1972). No such simple closure assumption has yet been demonstrated for wind flow over uneven ground, but several theoretical models have recently been presented (Jackson and Hunt, 1975, Deaves, 1976) using the uniform flow closure assumption in this context. These analyses were restricted to hills of small slope. In both cases the slope restriction arose from the mathematics of the solutions themselves but it is doubtful whether the closure assumption, obtained effectively for uniform flow, would remain valid for more severe slopes. An important result which emerged from the matched asymptotic analysis of Jackson and Hunt was that the action of the Reynolds stresses appeared to be significant only within a small inner layer close to the ground. This raises the possibility of seeking a solution to the problem by neglecting altogether the action of the Reynolds stresses and considering only the effects of the convective terms. Hopefully such a solution may give an adequate representation of the flow except within a thin layer close to the ground. This approach forms the basis of the analysis presented in this paper and the predicted values of wind speed correspond well to measured velocity profiles from wind tunnel models, and field measurements.

2 THE EQUATIONS

In this paper two dimensional configurations only are considered. It is assumed that the atmospheric boundary layer upwind of the hill has a prescribed velocity profile and hence a known vorticity distribution. It is also assumed that the hill is sufficiently low for Coriolis and buoyancy effects to be negligible throughout the solution region, i.e. the present solution is proposed only for low hills that lie well within the neutrally stable atmospheric shear layer close to the earth's surface.

The solution region and its boundaries are shown in figure (1). Boundaries C_1 and C_2 are taken at a large distance upstream and downstream of the hill and it is assumed that mean flow has no vertical component at these stations. It is also assumed that the horizontal velocity profile $u = u_o(y)$ is known on the upstream boundary. The ground elevation is defined by the surface C_3 and it is assumed that a control surface C_4, at a large height above the ground, acts as a stream surface forming a ceiling for the solution region.

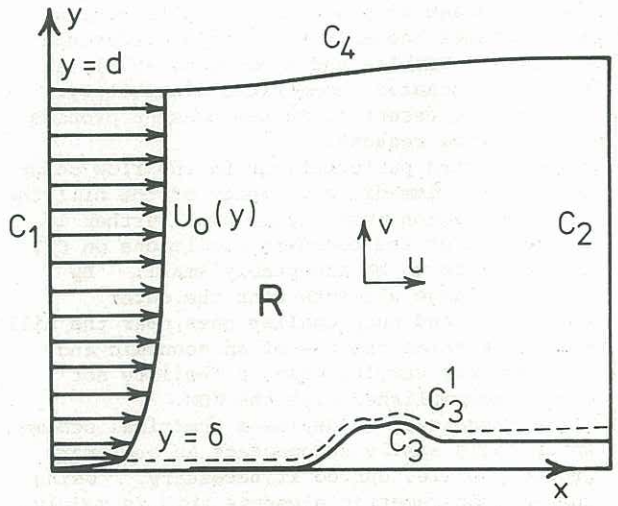

Figure (1) The solution region and boundaries

The horizontal and vertical mean wind velocities are defined in terms of a stream function ψ where;

$$u = \frac{\partial \psi}{\partial y}, \quad v = -\frac{\partial \psi}{\partial x} \tag{1}$$

It is assumed that the Reynolds stress terms are negligible throughout the region, as are the viscous stresses. Vorticity is then convected along streamlines and a vorticity equation results of the form;

$$\nabla^2 \psi = \psi_{xx} + \psi_{yy} = -\omega_o(\psi), \tag{2}$$

where $\omega_o(\psi)$ is defined implicitly by conditions at the upstream boundary, viz:

$$\omega_o = -\frac{\partial u_o}{\partial y}, \tag{3(a)}$$

$$\psi = \int_o^y u_o(y)dy. \qquad (3(b))$$

In terms of the stream function ψ the boundary conditions on the upstream and downstream boundaries become;

$$\psi_x = 0 \text{ on } C_1 \text{ and } C_2 \qquad (4)$$

On C_4 and C_3 ψ has constant values of 0 and ψ_d, i.e.

$$\psi = \psi_d = \int_o^d u_o(y)dy \text{ on } C_4, \qquad (5)$$

$$\psi = 0 \qquad \text{on } C_3 \qquad (6)$$

To avoid the presence of large variations in vorticity close to the ground the boundary C_3 is replaced by a boundary C_3' raised a small distance δ above the ground surface. In the results presented in this paper δ was taken to be of order 10 x y_o where y_o is the roughness length. We thus assume that a streamline exists close to the ground just above the local roughness elements. It is found that the solution is insensitive to δ. The boundary condition on C_3' replacing that on C_3 is then given by

$$\psi = \psi_\delta = \int_o^\delta u_o(y)dy \qquad (6(a))$$

The problem then reduces to the solution of equation (2) within the region R, bounded by C_1, C_2 C_3' and C_4.

The boundary conditions for ψ are then given by equations (4), (5) and (6a), and the function $\omega_o(\psi)$, occurring in equation (2) is defined implicitly by equation (3).

3 THE SOLUTION METHOD

A numerical solution to the above problem was obtained using the finite element method, (FEM). The FEM was chosen in preference to alternative numerical schemes, notably the finite difference method, (FDM), (Taublee and Robertson, 1972), as the FEM offers greater geometrical flexibility. This property is essential in the present problem for the following reasons;

(i) Though severe purturbations in the flow occur only in the immediate vicinity of the hill the solution region must extend much further if the effect of the boundary conditions on C_1, C_2 and C_4 is to be acceptably small. By choosing large elements near the outer boundaries and much smaller ones near the hill the FEM enables the use of an economic and continuously varying mesh, a facility not easily accomplished with the FDM.

(ii) It was necessary to devise a numerical scheme which could easily accommodate an arbitrary ground profile, curved if necessary. Using curved isoparametric elements this is simply achieved with the FEM. With the FDM a 'saw tooth' approximation would be required near the ground and the task of automatically generating suitable meshes for arbitrary ground profiles would be difficult if not impossible.

A Galerkin approach was used to formulate the problem in terms of finite elements. An outline of this process follows:

An approximate solution ψ' of equation (2) is sought where ψ' is a linear combination of a complete set of functions W_i ($i = 1, \cdots N$), as yet unspecified. ψ' is chosen so that it identically satisfies the hard boundary conditions on C_3' and C_4, i.e. $\psi' = \psi_\delta$ on C_3' and $\psi' = \psi_d$ on C_4. The residuals of equations (2) and boundary conditions (4) are then denoted by R_1, R_2 and R_3, i.e.

$$\nabla^2\psi' + \omega_o(\psi') = R_1 \quad \text{in R}, \qquad (7)$$

$$\psi_x' = R_2 \text{ on } C_1, \ \psi_x' = R_3 \text{ on } C_2. \qquad (8)$$

The residuals are then constrained to be zero when weighted with the functions W_i over R, C_1 and C_2 respectively giving;

$$\int_R (\nabla^2\psi' + \omega_o(\psi'))\, W_i \, dxdy = 0, \ (i = 1 \cdots N), \qquad (9)$$

$$\int_{C_1} \psi_x' W_i dy = 0, \ (i = 1, \cdots N), \qquad (10)$$

$$\int_{C_2} \psi_x' W_i dy = 0, \ (i = 1, \cdots N). \qquad (11)$$

Equation (9) may be rewritten;

$$\int_R (\psi_x' W_{i_x} + \psi_y' W_{i_y} - \omega_o(\psi')W_i)dxdy - \int_{C_1+C_2+C_3'+C_4} W_i \underline{\nabla}\psi' \cdot \hat{\underline{n}} ds = 0, \ (i = 1, \cdots N), \qquad (12)$$

where $\hat{n}$ is an outward unit normal vector.
W_i will be chosen so that $W_i \equiv 0$ on C_3' and C_4. Equation (12) then reduces to;

$$\int_R (\psi_x' W_{i_x} + \psi_y' W_{i_y} - \omega_o(\psi')W_i)dxdy = 0, \quad (i = 1, \cdots N). \qquad (12(a))$$

The region R is now divided into a number of elements defined by M nodes. The nodes are numbered 1, $\cdots$ M in such a way that the first N nodes do not lie on C_3' or C_4, (N < M). ψ is then defined at any point in R by a matrix equation;

$$\psi = [N(x, y)]\,\{\psi\} \qquad (13)$$

where $[N(x, y)] = [N_1, N_2 \cdots N_M]$ and $\{\psi\} = \{\psi_1, \psi_2 \cdots \psi_m\}^T$. ψ_i is value of ψ at the i^{th} nodal point and N_i is the shape function for that point defined implicitly inside each element by the appropriate component of an explicit element shape matrix. The values of ψ_i, $i = 1, \cdots N$, are unknown but the values of ψ_i, $i = N + 1, \cdots M$, are assumed known and are given by either ψ_d or ψ_δ. This automatically satisfies the previously assumed boundary conditions that $\psi' = \psi_d$ on C_4 and $\psi' = \psi_\delta$ on C_3'. The weight functions W_i are now chosen so that $W_i = N_i$, $i = 1, \cdots N$. This choice automatically satisfies the condition that $W_i \equiv 0$ on C_3' and C_4. Substituting into equation (12(a)) then gives the matrix equation

$$[K]\,\{\psi\} = \{F(\psi)\} \qquad (14)$$

where;

$$K_{ij} = \int_R (N_{i_x}N_{j_x} + N_{i_y}N_{j_y})\, dxdy, \ i=1,\cdots N, j=1,\cdots M \qquad (15)$$

and

$$F_i = \int_R \omega_o(\psi)N_i \, dy, \ i = 1, \cdots M. \qquad (16)$$

The matrices [K] and {F} are assembled from the appropriate element submatrices in the usual way, (Zienkiewicz, 1971).
Equation (14) may then be solved for the unknown nodal values of ψ using an iterative scheme;

$$[K]\,\{\psi_{n+1}\} = \{F(\psi_n)\}, \qquad (17)$$

where ψ_{n+1} and ψ_n are successive approximations to ψ. The improved values of ψ are then used to re-evaluate $\{F(\psi)\}$ from equation (16). Convergence is achieved when the fractional difference between successive approximations is acceptably small. Eight noded rectangular isoparametric elements were used with sixteen point numerical Gaussian integration within each element. Equation (17) was solved using a direct Gaussian elimination symmetric matrix solver. The solution may be greatly accelerated by the choice of an optimal node numbering scheme which minimises semi-bandwidth of the coefficient matrix.

4 RESULTS

Using the method described in the previous section FEM results were computed for escarpments with slopes 1:1, 1:2 and 1:4. These particular

topologies were chosen since extensive wind tunnel measurements are already available for comparison. (Bowen and Lindley, 1977). The 1:2 slope escarpment is of particular interest since field measurements for an escarpment of this form are also available, (Bowen and Lindley, 1974).

In each case the finite element model comprised 200 elements with 661 nodes. The 'ceiling' C_4 was placed twenty escarpment heights above the ground surface. Variation of C_4 by five escarpment heights above and below this level caused no appreciable modification in the computed results. The upstream and downstream boundaries C_1 and C_2 were of the order of ten escarpment heights upstream and downstream of the escarpment. The solution was found to be insensitive to displacement of C_1 and C_2 to positions further upstream and downstream respectively. A portion of the finite element mesh in the region near to the 1:2 slope escarpment is shown in figure (2). This illustrates the flexibility of mesh size which is available with the FEM. The topology of a typical element and its constitutive nodes is also shown in figure (2).

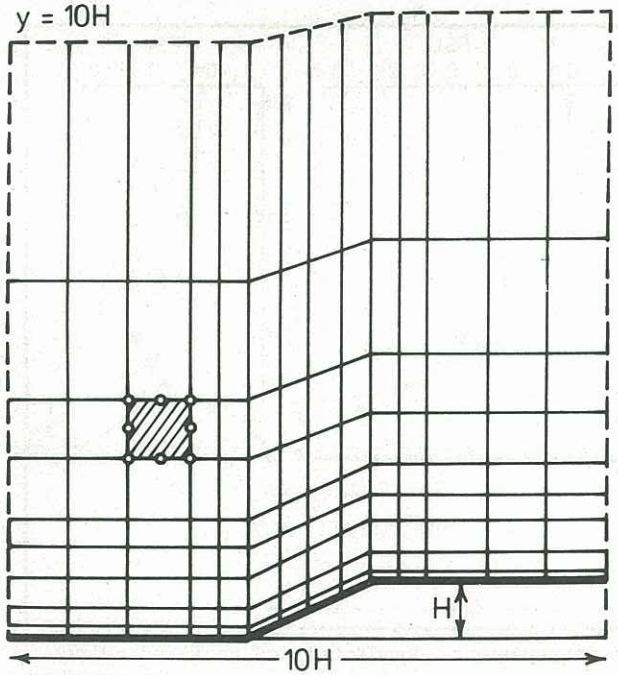

Figure (2) A portion of the finite element mesh near a 1:2 slope escarpment

The wind tunnel results were obtained from a 1:300 scale atmospheric boundary layer tunnel which closely approximated a power law velocity profile of the form;

$$u_o(y) = Ay^{\alpha}, \qquad (18)$$

with α equal to 1/6. The profile was created by roughness elements of height 0.06H, where H was the escarpment height, corresponding to a roughness length y_o of approximately 0.006H. FEM results were computed for an incident profile given by equation (18). Results were also computed for the corresponding log profile with $y_o = 0.006H$. The results were almost identical and only the 1/6 power law results are presented in this paper. The field measurements for the 1:2 slope escarpment were taken in a rural boundary layer near Christchurch, New Zealand. The upstream profile in this case was much flatter than that produced in the wind tunnel, approximating to a power law profile with $\alpha = 0.0816$. For comparison with these field measurements an FEM power law solution was computed with $\alpha = 0.0816$. A solution was also computed for the irrotational case, $\alpha = 0$.
In all cases convergence of the numerical scheme occurred after 4 - 6 iterations, representing a CPU time of 480 - 600 seconds on a Burroughs B6718 computer. The convergence criterion used was that;

$$\max \left| \left(\frac{\psi_{n+1} - \psi_n}{\psi_n} \right) \right| < 10^{-3}.$$

The results are shown in figures (3), (4) and (5). The results are presented in the form of computed and measured values of the fractional speed up (FSU) at various stations upstream and downstream of the escarpment. The FSU is defined by;

$$FSU = \frac{\tilde{u}(y) - u_o(y),}{u_o(y)}$$

where $\tilde{u}(y)$ is the total wind velocity at a height y above the local ground level. FSU is thus a relatively sensitive measure of velocity differences.

It can be seen that in all cases a good correspondence exists between the measured wind tunnel data and the appropriate FEM computations. This is particularly so at the base and crest of the escarpments where the FSU attains its minimum and maximum values. Downstream of the crest the effects of the surface roughness, which are neglected in this theory, cause the FSU to decrease near the ground. Even in this region, however, the FSU is well approximated by the current theory one hill height or more above the ground surface. It is of interest to note that the apparent disparity between the field measurements and wind tunnel data is predicted in this theory by the substantial difference in FSU for the two vorticity distributions given by $\alpha = 1.6$ and $\alpha = 0.0816$.

5 CONCLUSIONS

A finite element frozen vorticity solution for wind flow over hills has been shown to give results that are closely comparable over a large region of the flow with wind tunnel measurements and field data for the limited number of cases so far examined. These results appear to confirm the hypothesis that the flow is dominated by the convective effects and in particular the upstream vorticity profile. Further wind tunnel and field tests are now in progress to test the numerical scheme on more general ground topologies.

6 REFERENCES

BOWEN, A.J. and LINDLEY, D. (1977). 'A wind tunnel investigation of the wind speed and turbulence characteristics over various escarpment shapes', to be published J. of Boundary Layer Meteorology, 1977.

BOWEN, A.J. and LINDLEY, D. (1974). 'Measurements of the mean wind flow over various escarpment shapes', Proc. of the Fifth Australasian Conf. on Hydraulics and Fluid Mechanics, Christchurch, New Zealand, 1974. Vol. 1, pp 211-219.

DEAVES, D.M. (1976). 'Wind flow over hills: A numerical approach", Journal of Industrial Aerodynamics, 1976, 1, pp 371-391.

ESDU 72026 (1972). 'Characteristics of wind speed in the lower layers of the atmosphere near the ground: Strong winds (neutral atmosphere)'. Engineering Sciences Data Unit, London, 1972.

JACKSON, P.S. and HUNT, J.C.R., (1975). 'Turbulent wind flow over a low hill'. Quart. J. Royal Meteor. Soc., 1975, 101, pp 929-955.

TAUBLEE, D.B. and ROBERTSON, J.M. (1972).'Turbulent separation analysis ahead of a step'. Trans. A.S.M.E., Vol. 94, 1972, Series I, pp 544-550.

ZIENKIEWICZ, O.C. 'The finite element method in Engineering Science', McGraw-Hill, London, 1971.

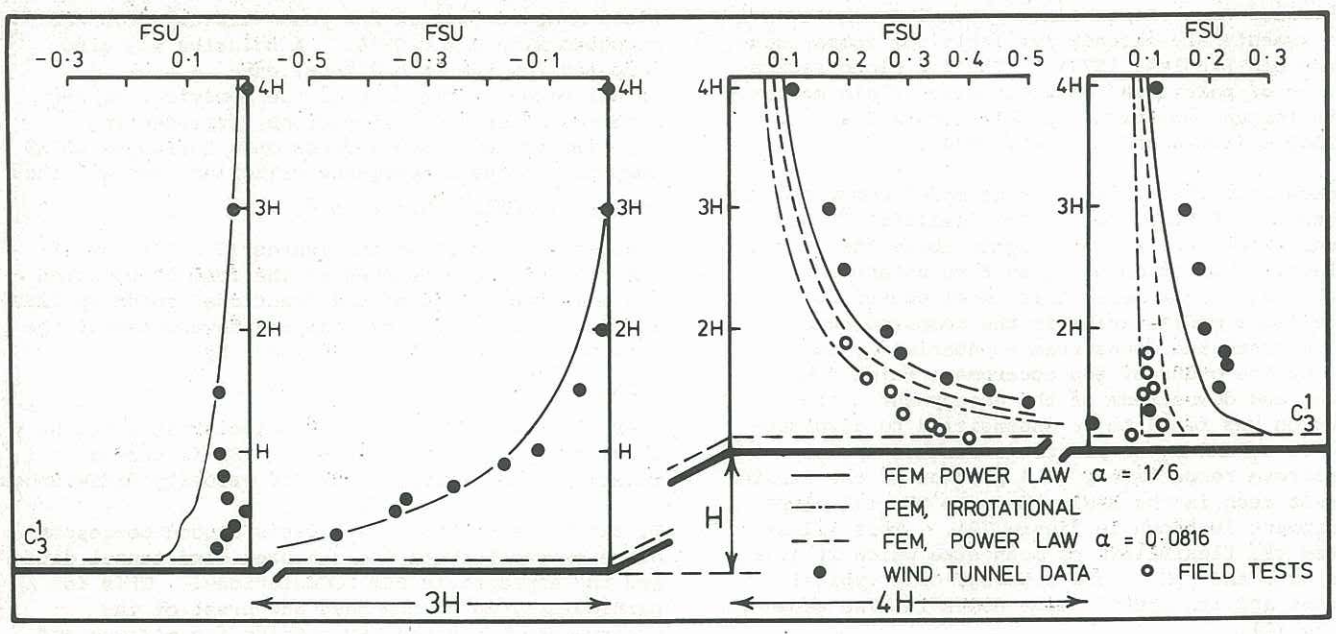

Figure (3) The variation of FSU with height for a 1:2 slope escarpment. Predicted and measured values.

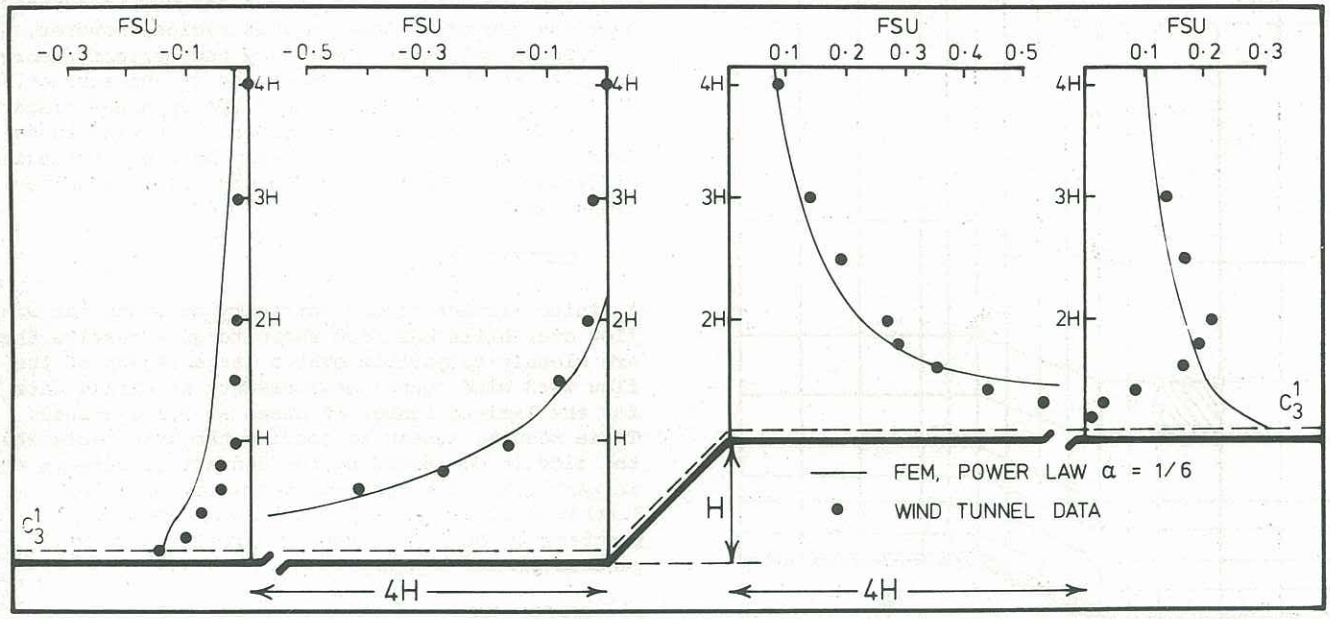

Figure (4) The variation of FSU with height for a 1:1 slope escarpment. Predicted and measured values.

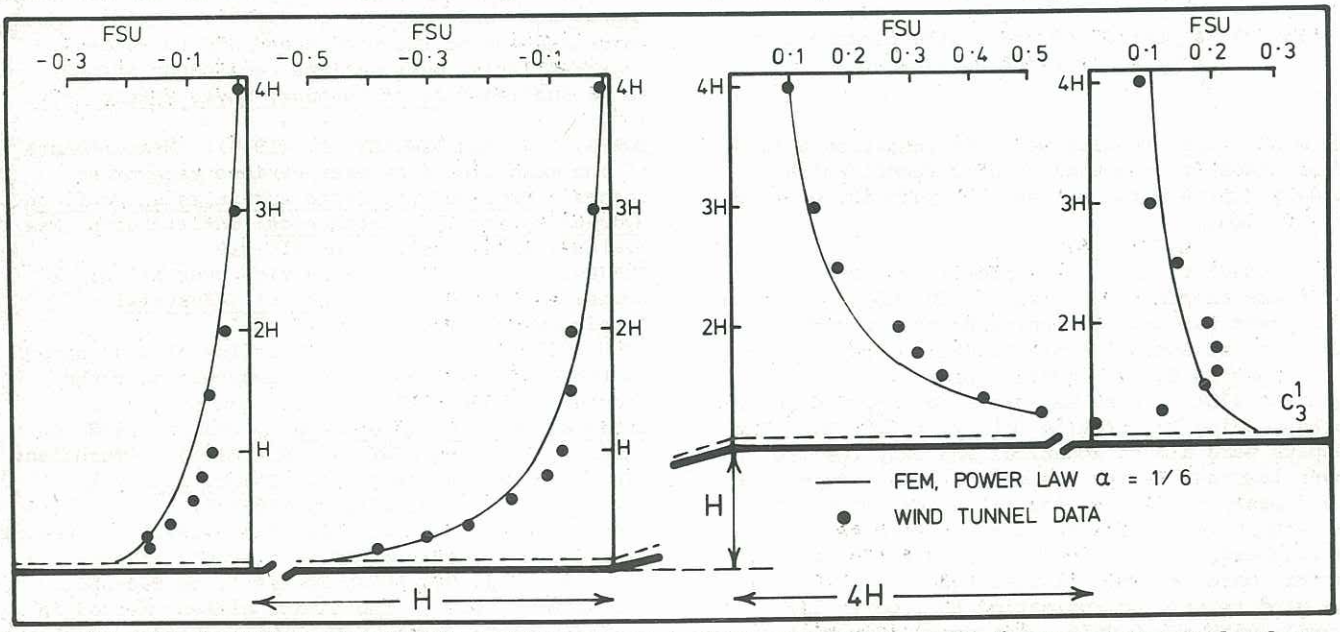

Figure (5) The variation of FSU with height for a 1:4 slope escarpment. Predicted and measured values.